Atomic Layer Deposition of Platinum Oxide and Metallic Platinum Thin Films from $Pt(acac)_2$ and Ozone

Jani Hämäläinen,*,† Frans Munnik,‡ Mikko Ritala,† and Markku Leskelä†

Laboratory of Inorganic Chemistry, Department of Chemistry, P.O. Box 55, FI-00014 University of Helsinki, Finland, and Institute of Ion Beam Physics and Materials Research, Forschungszentrum Dresden-Rossendorf, P.O. Box 510119, D-01314 Dresden, Germany

Received April 30, 2008. Revised Manuscript Received August 15, 2008

Platinum oxide and platinum thin films have been grown by atomic layer deposition (ALD) using $Pt(acac)_2$ (acac = acetylacetonato) and ozone as precursors. Amorphous platinum oxide thin films were deposited at 120 and 130 °C while metallic platinum films were obtained at 140 °C and above. The sublimation temperature of $Pt(acac)_2$ set the low temperature limit for oxide film deposition. The platinum oxide films were successfully deposited on Al_2O_3 and TiO_2 adhesion layers, soda lime glass, and silicon substrate with native oxide on top. Platinum films were grown on Al_2O_3 adhesion layer. The platinum oxide had good adhesion to all tested surfaces, whereas metallic platinum films did not pass the common tape test. Resistivities of 50−60 nm thick platinum oxide films were between 1.5 and 5 Ω cm at 130 °C and could be varied with both precursor pulse lengths. The resistivity of about 110 nm thick metallic film deposited at 140 °C was about 11 $\mu\Omega$ cm. The platinum films deposited at higher temperatures suffered from deterioration of thickness uniformity. The platinum oxide films can be reduced in 5% H_2 gas under reduced pressure at room temperature to porous platinum structures.

Introduction

Platinum as a noble metal is very well-known from its attractive properties for many nanoscale applications. However, oxides of platinum have not been as extensively characterized and their applicability is quite limited compared to the metallic platinum. This is because of their limited stability against reduction. In general, platinum oxide exists in several crystalline stoichiometric compositions, namely, PtO, Pt_3O_4, and PtO_2. PtO_2 has further α- and β-phases. Interestingly, even Pt_2O[1] and PtO[2] have appeared in the scientific literature, so platinum seems to have quite versatile oxide composition chemistry. The different compositions of platinum oxides reflect on their properties and therefore the applicability of different stoichiometric forms varies accordingly.

Catalytic properties of platinum oxides have been examined in several papers. PtO_2 has been suggested as a catalyst for hydrosilylation of functionalized alkenes[3] and alkynes,[4] and for silylation of aryl halides.[5] Bulk platinum oxide phases have been studied for dissociative adsorption of methane and for oxidation of CO.[6] Only Pt_3O_4 showed high catalytic oxidation activity. In addition, α-PtO_2 has been examined for catalytic oxidations of ethanol[7] and CO.[8] The surface oxide on platinum was found to have higher catalytic reactivity toward CO than the original metallic surface.[8]

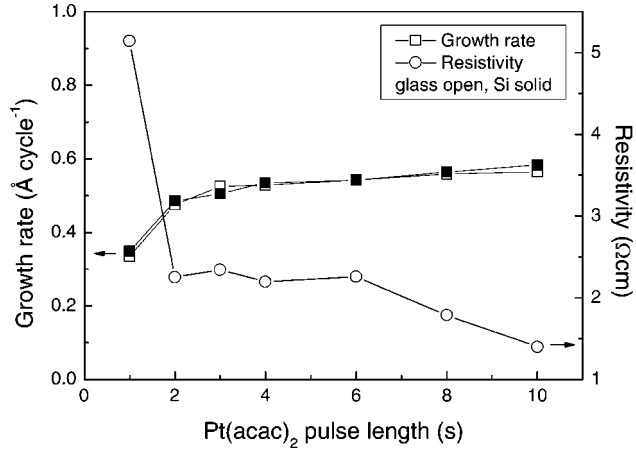

Figure 1. Growth rate, measured with XRR, and resistivity of PtO_X on soda lime glass and Si(111) substrates as a function of $Pt(acac)_2$ pulse length. The ozone pulse length was 2 s. 1000 cycles were applied at 130 °C.

The concentration of oxygen in platinum oxide affects its electrical properties. According to Abe et al.[9] PtO_X films with $X \leq 0.6$ have low resistivity with metallic conductivity. Therefore, low oxygen content platinum oxide films have been proposed as capacitor electrodes.[9,10] The resistivity of

* Corresponding author. E-mail: jani.hamalainen@helsinki.fi. Fax: 358 9 191 50198.
† University of Helsinki.
‡ Forschungszentrum Dresden-Rossendorf.

(1) Goto, M.; Kasahara, A.; Tosa, M. *Vacuum* **2006**, *80*, 740.
(2) Bare, W. D.; Citra, A.; Chertihin, G. V.; rews, L. *J. Phys. Chem.* **1999**, *103*, 5456.
(3) Sabouralt, N.; Mignani, G.; Wagner, A.; Mioskowski, C. *Org. Lett.* **2002**, *4*, 2117.
(4) Hamze, A.; Provot, O.; Brion, J.-D.; Alami, M. *Synthesis* **2007**, 2025.
(5) Hamze, A.; Provot, O.; Alami, M.; Brion, J.-D. *Org. Lett.* **2006**, *8*, 931.
(6) Seriani, N.; Pompe, W.; Ciacchi, L. C. *J. Phys. Chem. B* **2006**, *110*, 14860.
(7) Jin, Z.; Xi, C.; Zeng, Q.; Yin, F.; Zhao, J.; Xue, J. *J. Mol. Catal. A: Chem.* **2003**, *191*, 61.
(8) Ackermann, M. D.; Pedersen, T. M.; Hendriksen, B. L. M.; Robach, O.; Bobaru, S. C.; Popa, I.; Quiros, C.; Kim, H.; Hammer, B.; Ferrer, S.; Frenken, J. W. M. *Phys. Rev. Lett.* **2005**, *95*, 255505.
(9) Abe, Y.; Yanagisawa, H.; Sasaki, K *Jpn. J. Appl. Phys* **1998**, *37*, 4482.
(10) Huang, C.-K.; Chiou, Y.-K.; Chu, Y.-C.; Wu, T.-B.; Tsai, C.-J. *J. Electrochem. Soc.* **2006**, *153*, F115.

10.1021/cm801187t CCC: $40.75
Published on Web 10/08/2008

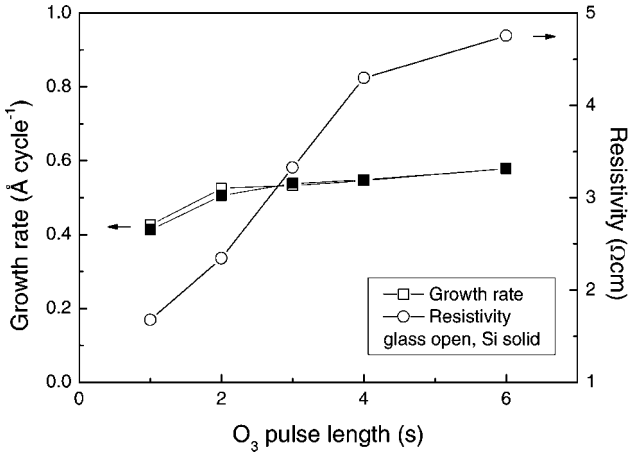

Figure 2. Growth rate and resistivity of PtO_X as a function of ozone pulse length. The $Pt(acac)_2$ pulse length was 3 s. 1000 cycles were applied at 130 °C.

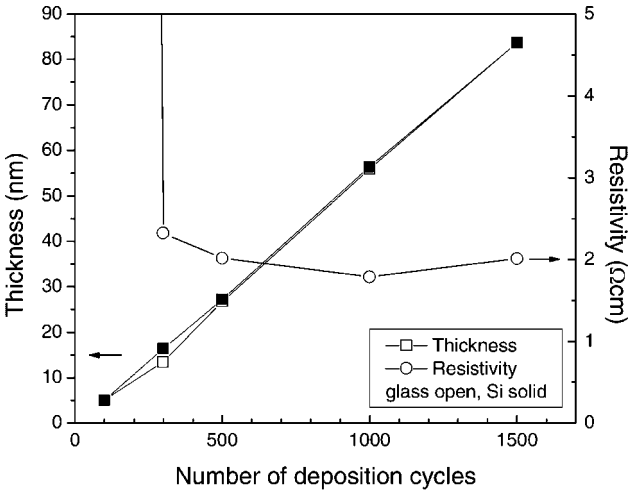

Figure 3. Thickness and resistivity of PtO_X as a function of number of deposition cycles. Pulse lengths for $Pt(acac)_2$ and ozone were 8 and 2 s, respectively. The films were deposited at 130 °C.

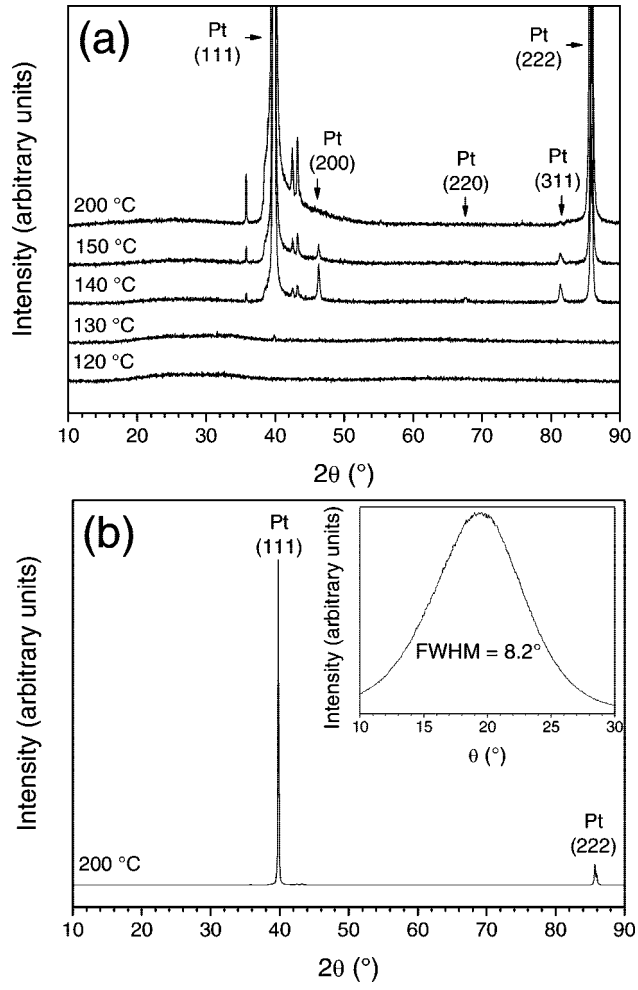

Figure 4. (a) XRD patterns of the films deposited at different temperatures and (b) the full XRD pattern of the Pt film deposited at 200 °C with the inset showing a rocking curve of the Pt(111) peak. 2000 cycles were applied in each process. Pulse lengths were 8 and 2 s for $Pt(acac)_2$ and ozone, respectively. The substrate was soda lime glass with an Al_2O_3 adhesion layer.

the films increases with increasing oxygen content, and the films with high oxygen content show semiconducting character.[9]

The ability to easily reduce platinum oxide films by impact of heat or by energetic ions makes platinum oxide an intriguing material for several applications. The super-resolution near-field structure (super-RENS), in which the diffraction limitations of a laser can be circumvented, is considered a promising technology to increase the data storage capacity of optical media. A thin PtO_X layer is often chosen as a mask or an active layer in super-RENS.[11−17] On the other hand, focused ion beam or laser irradiation can be applied to high resistivity platinum oxide for metallization, patterning or writing electrical connections to the films.[18−20] Interestingly, thermal decomposition behavior of platinum oxide has been proposed to be exploited even in a thermal lithography technique.[21] According to the authors, this approach would be useful for fabricating nanoscale structures with a high aspect ratio over large areas.

Nanoporous platinum oxide thin film has been reported as a hydrogen ion-selective sensing material, and thus suggested as a promising alternative to iridium oxide in pH sensors.[22] Porous structures for electrodes can be achieved by reduction of platinum oxide to metallic platinum either by exposure to hydrogen or by electrochemical means.[23]

(11) Li, X.; Kim, C. I.; An, S. H.; Oh, S. G.; Kim, S. Y *Jpn. J. Appl. Phys* **2005**, *44*, 3623.
(12) Qu, Q.-L.; Wang, Y.; Gan, F.-X. *Chin. Phys. Lett.* **2006**, *23*, 3363.
(13) Hwang, I.; Kim, J.; Kim, H.; Park, I.; Shin, D. *IEEE Trans. Magn.* **2005**, *41*, 1001.
(14) Kikukawa, T.; Fukuzawa, N.; Kobayashi, T. *Jpn. J. Appl. Phys.* **2005**, *44*, 3596.
(15) Qu, Q.; Wang, Y.; Gan, F. *Phys. Lett. A* **2007**, *368*, 271.
(16) Shima, T.; Yamakawa, Y.; Tominaga, J. *Jpn. J. Appl. Phys.* **2007**, *46*, L135.
(17) Liu, Q.; Fukaya, T.; Cao, S.; Guo, C.; Zhang, Z.; Guo, Y.; Wei, J.; Tominaga, J. *Opt. Express* **2008**, *16*, 213.
(18) Machalett, F.; Edinger, K.; Melngailis, J.; Venkatesan, T.; Diegel, M.; Steenbeck, K. *Appl. Phys. Lett.* **2000**, *76*, 3445.
(19) Machalett, F.; Edinger, K.; Diegel, M.; Steenbeck, K. *Microelectron. Eng.* **2002**, *60*, 429.
(20) Machalett, F; Gärtner, K.; Edinger, K.; Diegel, M *J. Appl. Phys.* **2003**, *93*, 9030.
(21) Kurihara, K.; Yamakawa, Y.; Nakano, T.; Tominaga, J. *J. Opt. A: Pure Appl. Opt.* **2006**, *8*, S139.
(22) Park, S.; Boo, H.; Kim, Y.; Han, J.-H.; Kim, H. C.; Chung, T. D. *Anal. Chem.* **2005**, *77*, 7695.
(23) Maya, L.; Brown, G. M.; Thundat, T. *J. Appl. Electrochem.* **1999**, *29*, 883.

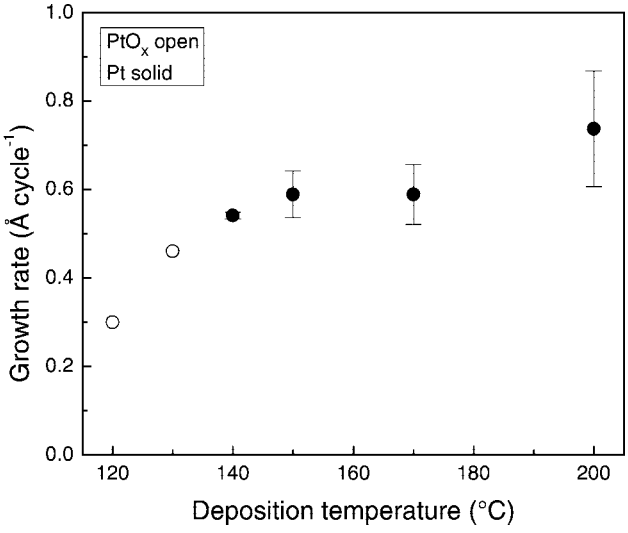

Figure 5. Growth rates of PtO_X and Pt films on Si substrates as a function of deposition temperature. A thin layer of Al_2O_3 was used as an adhesion layer. Pulse lengths were 8 and 2 s for $Pt(acac)_2$ and ozone, respectively. 2000 cycles were applied in each process. Film thicknesses were determined by EDX. The growth rates of the Pt films are average values calculated from the four thickness measurement points over the substrate. The error bars of the Pt films denote the standard deviations of the growth rate over the substrate.

Incorporation of platinum oxide into nanotubes has also been described in the literature.[24]

Platinum oxide thin films have been deposited mostly by physical methods. Sputtering[25−29] has been by far the most often used method to produce platinum oxide films with different stoichiometries. To form oxide layers on top of Pt surfaces, O_2 plasma treatment,[30] O_2 plasma immersion ion implantation,[31] and anodic polarization[32] have been employed.

Atomic layer deposition (ALD),[33−36] as one of the chemical vapor deposition (CVD) techniques, is an attractive thin film deposition method for applications where conformality, uniformity, thickness controllability and repeatability of the films have to be strictly met. Several thermal ALD processes for different noble metals, such as platinum,[37,38] ruthenium,[39−41] rhodium,[42] palladium,[43,44] and iridium,[45−47] have been developed in recent years. Additionally, silver has been grown by radical enhanced ALD.[48]

Thermal ALD noble metal processes employ mostly molecular oxygen as a reactive agent. In these processes molecular oxygen is dissociatively chemisorbed on the noble metal surface as atomic oxygen, partially diffusing into the subsurface region.[49,50] During the noble metal precursor pulse, a reaction takes place between the ligands of the metal precursor and the adsorbed oxygen atoms producing a metallic film. Each process requires a certain threshold temperature to proceed, being governed most likely by the dissociative chemisorption of O_2. Above the threshold temperature, the reaction between the adsorbed oxygen atoms and the metal precursor seems to be so fast that all oxygen becomes consumed and metallic film results instead of an oxide. However, if the deposition temperature can be lowered to the point where the oxygen atoms deposited in the film will not react with the metal precursor and a more oxidizing precursor is used, an oxide may form. Previously, we have reported ALD of iridium oxide films employing ozone.[51] At low deposition temperatures, IrO_2 was obtained whereas metallic Ir was formed at higher temperatures. Ozone is more reactive than O_2 and thus can create adsorbed oxygen atoms at such low temperatures where they do not become consumed in reactions with the metal precursor, thus resulting in an oxide film.

The suitability of the platinum precursor $Pt(acac)_2$ has been previously tested for ALD.[50,52,53] Utriainen et al.[52] noticed that the in-house synthesized $Pt(acac)_2$ decomposed during sublimation at 155 °C (0.6−1 mbar) and therefore the precursor could not be applied in a controlled manner. Aaltonen et al.[50,53] have examined the ALD platinum process using $Pt(acac)_2$ and molecular oxygen at the deposition

(24) Ma, X.; Feng, C.; Jin, Z.; Guo, X.; Yang, J.; Zhang, Z. *J. Nanopart. Res.* **2005**, *7*, 681.
(25) Abe, Y.; Kawamura, M.; Sasaki, K *Jpn. J. Appl. Phys* **1999**, *38*, 2092.
(26) Neff, H.; Henkel, S.; Hartmannsgruber, E.; Steinbeiss, E.; Michalke, W.; Steenbeck, K.; Schmidt, H. G. *J. Appl. Phys.* **1996**, *79*, 7672.
(27) Aita, C. R. *J. Appl. Phys.* **1985**, *58*, 3169.
(28) Maya, L.; Riester, L.; Thundat, T.; Yust, C. S. *J. Appl. Phys.* **1998**, *84*, 6382.
(29) Shima, T.; Tominaga, J *Jpn. J. Appl. Phys* **2003**, *42*, 3479.
(30) Blackstock, J. J.; Stewart, D. R.; Li, Z. *Appl. Phys. A: Mater. Sci. Process.* **2005**, *80*, 1343.
(31) Chen, Y.-C.; Sun, Y.-M.; Yu, S.-Y.; Hsiung, C.-P.; Gan, J.-Y.; Kou, C.-S. *Nucl. Instrum. Methods Phys. Res., Sect. B* **2005**, *237*, 296.
(32) Alsabet, M.; Grden, M.; Jerkiewicz, G. *J. Electroanal. Chem.* **2006**, *589*, 120.
(33) Ritala, M. ; Leskelä, M. In *Handbook of Thin Film Materials*; Nalwa, H. S., Ed.; Academic Press: San Diego, CA, 2001; Vol. 1, pp 103−159.
(34) Puurunen, R. L. *J. Appl. Phys.* **2005**, *97*, 121301.
(35) Elers, K.-E.; Blomberg, T.; Peussa, M.; Aitchison, B.; Haukka, S.; Marcus, S. *Chem. Vap. Deposition* **2006**, *12*, 13.
(36) Leskelä, M.; Aaltonen, T.; Hämäläinen, J.; Niskanen, A.; Ritala, M. *Proc. Electrochem. Soc.* **2005**, *545*, 2005–09.
(37) Aaltonen, T.; Ritala, M.; Sajavaara, T.; Keinonen, J.; Leskelä, M *Chem. Mater.* **2003**, *15*, 1924.
(38) Aaltonen, T.; Ritala, M; Tung, Y.-L.; Chi, Y.; Arstila, K.; Meinander, K.; Leskelä, M. *J. Mater. Res.* **2004**, *19*, 3353.
(39) Aaltonen, T.; Alén, M; Ritala, M.; Leskelä, M *Chem. Vap. Deposition* **2003**, *9*, 45.
(40) Aaltonen, T.; Ritala, M.; Arstila, K.; Keinonen, J.; Leskelä, M. *Chem. Vap. Deposition* **2004**, *10*, 215.
(41) Biener, J.; Baumann, T. F.; Wang, Y.; Nelson, E. J.; Kucheyev, S. O.; Hamza, A. V.; Kemell, M.; Ritala, M.; Leskelä, M. *Nanotechnology* **2007**, *18*, 055303.
(42) Aaltonen, T.; Ritala, M.; Leskelä, M. *Electrochem. Solid-State Lett.* **2005**, *8*, C99.
(43) Ten Eyck, G. A.; Pimanpang, S.; Bakhru, H.; Lu, T.-M.; Wang, G.-C. *Chem. Vap. Deposition* **2006**, *12*, 290.
(44) Elam, J. W.; Zinovev, A.; Han, C. Y.; Wang, H. H.; Welp, U.; Hryn, J. N.; Pellin, M. J. *Thin Solid Films* **2006**, *515*, 1664.
(45) Aaltonen, T.; Ritala, M; Sammelselg, V.; Leskelä, M. *J. Electrochem. Soc.* **2004**, *151*, G489.
(46) Färm, E.; Kemell, M.; Ritala, M.; Leskelä, M. *Chem. Vap. Deposition* **2006**, *12*, 415.
(47) Kemell, M.; Pore, V.; Ritala, M.; Leskelä, M. *Chem. Vap. Deposition* **2006**, *12*, 419.
(48) Niskanen, A.; Hatanpää, T.; Arstila, K.; Leskelä, M.; Ritala, M. *Chem. Vap. Deposition* **2007**, *13*, 408.
(49) Aaltonen, T.; Rahtu, A.; Ritala, M.; Leskelä, M. *Electrochem. Solid-State Lett.* **2003**, *6*, C130.
(50) Aaltonen, T. Ph.D. thesis, University of Helsinki, Helsinki, Finland, 2005; available from http://ethesis.helsinki.fi/en/.
(51) Hämäläinen, J.; Kemell, M.; Munnik, F.; Kreissig, U.; Ritala, M.; Leskelä, M *Chem. Mater.* **2008**, *20*, 2903.
(52) Utriainen, M.; Kröger-Laukkanen, M.; Johansson, L-S.; Niinistö, L. *Appl. Surf. Sci.* **2000**, *157*, 151.
(53) Aaltonen, T.; Ritala, M. ; Leskelä, M. Atomic Layer Deposition of Noble Metals. In *Advanced Metallization Conference 2004 (AMC 2004)*, San Diego, CA, Oct 19−21, 2004, and Tokyo, Sept 28−29, 2004; Erb, D., Ramm, P., Masu, K., Osaki, A. , Eds.; Materials Research Society, Warrendale, PA, 2005; pp 663−667.

Table 1. Elemental Compositions of the Platinum Oxide and Metallic Platinum Films Deposited between 120 and 200 °C as Measured with ERDA[a]

dep. temp. (°C)	H (at %)	C (at %)	O (at %)	Pt (at %)	O/Pt ratio
120	5.69 ± 0.08	1.6 ± 0.2	33.5 ± 1.0	59.2 ± 0.1	0.55 < *X* < 0.58
130	4.99 ± 0.06	<0.5	34.4 ± 0.8	60.6 ± 0.1	0.55 < *X* < 0.58
140	0.65 ± 0.01	<0.5	5.8 ± 0.4	93.6 ± 0.1	0.06
150	0.46 ± 0.01	<0.5	5.7 ± 0.3	93.8 ± 0.1	0.06
200	0.38 ± 0.01	<0.5	8.3 ± 0.5	91.3 ± 0.1	0.09

[a] The uncertainties in the table are only statistical uncertainties excluding possible systematic errors.

Table 2. Elemental Compositions of the Platinum Oxide Films Deposited at 120 and 130 °C as Measured with ERDA and Corrected for the Elemental Loss[a]

dep. temp. (°C)	dose	H (at %)	C (at %)	O (at %)	Pt (at %)	O/Pt ratio
120	half	13.1 ± 0.6	<0.5	47.8 ± 4.8	39.2 ± 0.6	1.09 < *X* < 1.35
120	full	13.5 ± 0.5	<0.5	49.1 ± 4.7	37.4 ± 0.6	1.18 < *X* < 1.44
130	half	10.5 ± 0.4	<0.5	54.7 ± 3.2	34.8 ± 0.6	1.47 < *X* < 1.67
130	full	10.3 ± 0.4	<0.5	54.8 ± 3.0	34.9 ± 0.6	1.48 < *X* < 1.66

[a] The uncertainties in the table comprise the statistical uncertainties in the measurement and the uncertainties in the extrapolation to zero dose.

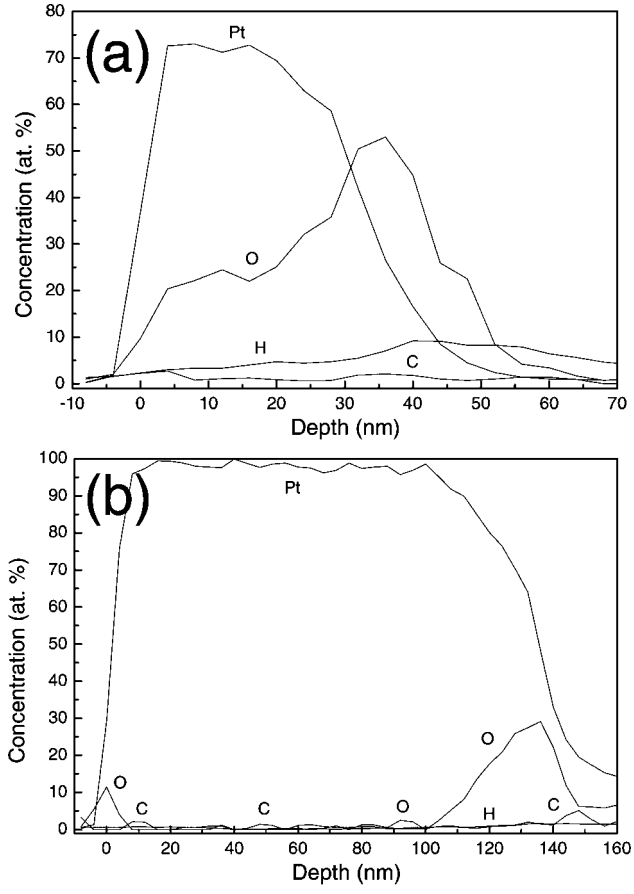

Figure 6. ERDA depth profiles of the films deposited at (a) 120 and (b) 140 °C.

temperatures of 210−220 °C. $Pt(acac)_2$ was sublimed at lower temperature (120 °C at about 10 mbar) than in the earlier study, but the films grown were nonuniform because of the poor thermal stability of the platinum precursor. In the successful platinum ALD process, (methylcyclopentadienyl)trimethylplatinum ($MeCpPtMe_3$) was used as the precursor.[37,38] $MeCpPtMe_3$, however, is substantially more expensive than $Pt(acac)_2$.

In this work, we concentrate on the preparation of amorphous platinum oxide thin films by ALD from $Pt(acac)_2$ and ozone. Uniform films can be obtained by choosing proper $Pt(acac)_2$ sublimation temperature and by employing more reactive oxidizing agent than molecular oxygen. To the best of our knowledge, this is the first time a chemical vapor deposition technique has been successfully applied for the deposition of platinum oxide films. Additionally, it is also shown that with these precursors, metallic platinum can be deposited at temperatures lower than those used in the earlier ALD Pt process.[37,38]

Experimental Section

Platinum oxide thin films were deposited in a hot-wall flow-type F-120 ALD reactor (ASM Microchemistry Ltd., Finland) operated under a nitrogen pressure of about 10 mbar. Nitrogen (99.9995%) was produced with a NITROX UHPN 3000 nitrogen generator and used as a carrier and a purging gas. Silicon (111) and soda lime glass substrates (5 × 5 cm^2) were ultrasonically cleaned in alkaline solution at 50 °C, followed by ultrasonic baths of ethanol and deionized water at room temperature for 10 min each. The substrates were next rinsed with deionized water and 50% ethanol, blown dry with nitrogen, and then stored for later use. Prior to loading into the reactor the substrates were rinsed with ethanol and blown dry with nitrogen to remove dust particles. In some cases before deposition of platinum oxide, a thin layer of Al_2O_3 was deposited in situ on the substrates by ALD using trimethylaluminum (TMA) and water.[34] $Pt(acac)_2$ (Volatec, Finland, and Alfa Aesar) was sublimed from an open boat held inside the reactor at 110 °C. Ozone was produced with a Wedeco Ozomatic Modular 4 HC ozone generator from oxygen (99.999% and 99.9999%, Linde Gas) and pulsed into the reactor through a needle valve and a solenoid valve from the main ozone flow line. The estimated ozone concentration output of the generator was about 100 g/Nm^3. The deposition temperature range studied was from 120 to 200 °C. Pulses for $Pt(acac)_2$ and ozone were varied up to 10 and 6 s, respectively. Each precursor pulse was followed by a 1 s nitrogen purge. Platinum oxide was deposited also onto a trench patterned silicon substrate using 5 s pulses and purges for conformality testing.

Film structures were identified from X-ray diffraction (XRD) patterns measured with a PANanalytical X'Pert Pro diffractometer. Film thicknesses were determined from X-ray reflectivity (XRR) patterns measured with a Bruker AXS D8 Advance X-ray diffractometer and by energy-dispersive X-ray spectroscopy (EDX). The EDX spectra were obtained using an Oxford INCA 350 mi-

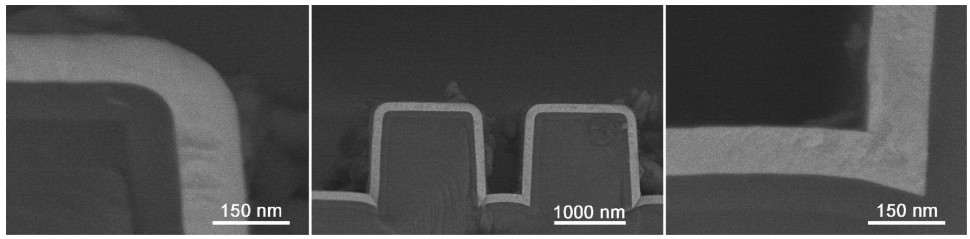

Figure 7. FESEM images of the PtO_X film deposited at 120 °C on trench patterned Si substrate. 2500 cycles were applied using 5 s pulses and purges for both precursors.

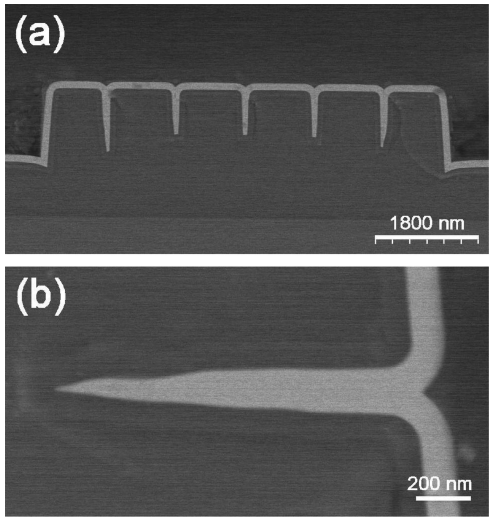

Figure 8. FESEM images (a) and (b) of the PtO_X film deposited onto narrow trenches. The growth parameters are the same as in Figure 7.

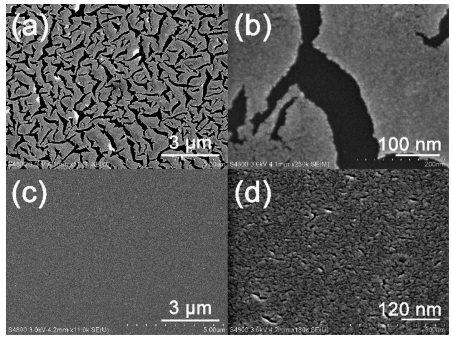

Figure 9. FESEM images of about (a, b) 14 and (c, d) 95 nm thick PtO_X films reduced to metallic Pt under 5% H_2 flow at room temperature for a day.

croanalysis system connected to a Hitachi S-4800 field emission scanning electron microscope (FESEM). The spectra were analyzed using a GMR electron probe thin film microanalysis program.[54] Thin film morphology was examined by the FESEM. Resistivities of the platinum oxide thin films were calculated from sheet resistances measured with a four-point probe technique and from the film thicknesses. Adhesion of the films to the substrates was tested with a simple Scotch tape test. Elemental compositions and depth profiles of the films were determined with elastic recoil detection analysis (ERDA) using a 35 MeV Cl^{7+} ion beam.[55]

Results and Discussion

Figure 1 shows the growth rate and resistivity of the PtO_X as a function of the $Pt(acac)_2$ pulse length. The growth rate is about 0.5 Å/cycle with 2 s $Pt(acac)_2$ pulse length and slightly increases close to 0.6 Å/cycle when 10 s pulses are used. EDX verified that this increase is due to more platinum being deposited with increasing $Pt(acac)_2$ pulse length. Thus the process is closely but not purely self-limiting. The decrease in resistivity also suggests a small change in film composition. With the shortest $Pt(acac)_2$ pulses, the reactions may be less complete, leaving more impurities in the film. Though the film grown with 1 s $Pt(acac)_2$ pulse is thinner (~35 nm) than the others (50−60 nm), the thickness hardly can explain the higher resistivity as the thickness effect becomes important only below 15 nm (see Figure 3 below).

The effect of ozone pulse length on the growth rate and on the resistivity is presented in Figure 2. A small increase in the growth rate with increasing pulse length is observed similar to Figure 1, but the ozone pulse length has a greater impact on the resistivity than the $Pt(acac)_2$ pulse length. The resistivity increases from about 2.5 to 4.8 Ω cm as the ozone pulse is increased from 2 to 6 s. Changes in the ratio between oxygen and platinum contents (see below) are most likely the cause for the large resistivity changes when the pulse lengths of each precursor are varied.

The film thickness seems to depend linearly on the number of the deposition cycles (Figure 3). The slope of the linear plot verifies a growth rate of about 0.55 Å/cycle. The growth rates are identical on Si(111) and soda lime glass substrates. For 25 nm and thicker films deposited at 130 °C, the resistivity stabilizes to about 2 Ω cm when the pulse lengths for $Pt(acac)_2$ and ozone are 8 and 2 s, respectively.

The films are amorphous from 120 to 130 °C, whereas metallic Pt is formed at 140 °C and above according to XRD patterns (Figure 4a). ERDA results (to be discussed below) verified that the amorphous films were platinum oxide while the crystalline films contained only 6−8 at % oxygen. At 130 °C, a faint reflection at the Pt(111) peak position can be seen in the pattern, which may be related to a minor contribution of reduced phase. However, orthorhombic PtO_2 and cubic Pt_3O_4 have reflections close to the Pt(111) reflection, so the origin of the reflection remains uncertain. The metallic Pt films have a polycrystalline structure with a strong (111) orientation (Figure 4b) similar to the films produced by ALD using $MeCpPtMe_3$ and molecular oxygen.[37,38] The difference to the reported ALD Pt films is that the film deposited in this work at 200 °C does not show any Pt(200), Pt(220), and Pt(311) reflections (a and b in Figure 4). The full width at half-maximum (fwhm) calculated from the rocking curve of the Pt(111) reflection was 8.2° (Figure 4b), which is lower than that in the earlier study (fwhm = 13°).[37]

(54) Waldo, R. A. *Microbeam Anal.* **1988**, *23*, 310.
(55) Kreissig, U.; Grigull, S.; Lange, K.; Nitzsche, P.; Schmidt, B. *Nucl. Instrum. Methods Phys. Res., Sect. B* **1998**, *674*, 136–138.

Growth rates of the films deposited between 120 and 200 °C (Figure 5) show that PtO_X growth rate increases from 0.3 Å/cycle close to 0.5 Å/cycle when the deposition temperature is increased from 120 to 130 °C. The film thicknesses as determined by EDX lead to a bit lower growth rates compared to the thicknesses obtained from XRR. The thickness difference was related to the nonstoichiometric films and the related uncertainty in density. The sublimation temperature of the platinum precursor, 110 °C, sets the low-temperature limit for the PtO_X deposition and the high-temperature limit is governed by the metallic form becoming more favorable similar to the ALD processes employing molecular oxygen. Metallic Pt films are obtained already at 140 °C, which is a considerably lower temperature than the deposition temperature of 200 °C in the previous study[38] using $MeCpPtMe_3$ and molecular oxygen. Also, the growth rate of the metallic Pt film at 140 °C is even higher than the largest reported growth rate of ALD Pt from $MeCpPtMe_3$ and molecular oxygen (0.5 Å/cycle at 300 °C).[38] On the other hand, as seen from Figure 5, the thickness uniformity across the film deteriorates at higher deposition temperatures.

The easy reduction of the platinum oxide under an energetic ion beam makes it a challenging material to be analyzed by ERDA. Tables 1 and 2 present elemental compositions of the films deposited between 120 and 200 °C using $Pt(acac)_2$ and ozone pulse lengths of 8 and 2 s, respectively. The films were deposited on an Al_2O_3 adhesion layer on top of Si substrates. The results are average atomic concentrations over the whole layer; however, the amount of oxygen coming from the Al_2O_3 adhesion layer and the native SiO_2 on top of the substrate has been estimated and subtracted from the results. Because of the lower detector resolution for hydrogen, the corresponding average atomic concentrations may also contain hydrogen from the underlying layers. The carbon and hydrogen contents of the metallic Pt films are similar to the ALD Pt process using molecular oxygen[37] but the oxygen concentration of about 6 at % is substantially higher than reported earlier (1.0 to 2.0 at %). In part this may be caused by the fact that the average oxygen concentration in the film is increased by the presence of oxygen at the interface (Figure 6b).

To compensate for the instant reduction of the PtO_X films upon ion beam irradiation, the ERDA measurements of these films have been analyzed with elemental loss compensation. Intermediate files were saved after each 1/20th portion of the total dose. The total counts for hydrogen, oxygen, and platinum were determined and plotted for each section of the dose. The platinum count was analyzed from scattered chlorine ions. The curves were fitted and extrapolated to zero doses for each element to obtain a correction for the elemental loss due to the reduction of the films caused by the ion beam. The extrapolation to zero dose can be made from different starting points. Two analyses per sample were made, for half-dose and for full dose, after which the correction for the elemental loss was applied. The corrected elemental compositions are presented in Table 2. The ratio between oxygen and platinum is much larger than in the results uncorrected for elemental loss (0.55) in Table 1; however, it is still nonstoichiometric. The oxygen to platinum ratios may still contain additional errors because of the elemental loss correction procedure that may lead to the quite low oxygen to platinum ratios.

Figure 6 contains the depth profiles of PtO_X and metallic Pt films. The depth profile for the oxide film (Figure 6a) represents the composition obtained for the full dose, including the elemental loss during the measurement. The sudden increase in oxygen concentration in the second half of the film is the result of the fact that the original resistive film is reduced from the surface during ion beam bombardment leaving more oxygen deeper in the sample. Additionally, the depth profiles presented in panels a and b in Figure 6 are convoluted with the system resolution and physical effects like straggling, which means that the actual depth profile can be much sharper than in the figures. Therefore, in the metallic film (Figure 6b), the rise of the oxygen content near the interface may be related to the Al_2O_3 adhesion layer.

As seen from Figure 3, the resistivity values of the platinum oxide films deposited at 130 °C are close to 2 Ω cm with an estimated stoichiometric structure of about $PtO_{1.6}$ (Table 2). Amorphous PtO_2 films deposited by sputtering at 300 and 40 °C have been reported to have resistivities of about 8 Ω cm and 3×10^2 to 3×10^3 Ω cm, respectively.[28] As there were no significant differences in stoichiometries between the film composition, the authors related the large variance in resistivities to the very small oxygen losses of about <0.1 wt %. For sputtered polycrystalline PtO and α-PtO_2 films, resistivities of $1-2 \times 10^{-3}$ Ω cm and about 1 Ω cm, respectively, have been reported.[25] By contrast Machalett et al.[19] have obtained similar resistivities of 2.2×10^{-3} Ω cm and $1.0-1.4 \times 10^{-3}$ Ω cm for stoichiometric PtO and PtO_2 films. These results show that platinum oxides have large variations in resistivities depending on growth parameters and stoichiometries. The resistivity of a 110 nm thick Pt film deposited at 300 °C by ALD was 12 μΩ cm when air was used.[37] A 30 nm thick film grown at 200 °C and a 50 nm thick film grown at 300 °C had resistivities about 17 μΩ cm and 13 μΩ cm, respectively.[38] In our study, the resistivity of about 110 nm thick Pt film deposited at 140 °C was about 11 μΩ cm.

Conformal growth was verified by depositing PtO_X on trench-structured Si substrate (Figure 7). PtO_X can also be used to fill the trenches completely when the film thickness is high enough compared to the trench width (images a and b in Figure 8). Relatively complex structures should be possible to be coated and filled by choosing proper film growth parameters.

When platinum oxide is exposed to 5% H_2 gas under reduced pressure, reduction to reflective, metallic films occur already at room temperature (Figure 9). The reaction is relatively slow, however. If the partial pressure of H_2 is higher, the reduction process is also faster. Images a and b in Figure 9 show how the large density difference between platinum oxide and metallic platinum causes discontinuity to a thin (originally 14 nm) film upon reduction. By contrast, when a thicker, 95 nm thick PtO_X is reduced, the resulting metallic film is quite smooth in appearance (images c and d in Figure 9). This kind of reductive treatments might be employed to alter material properties of the films and

facilitate low temperature approach to metallic platinum film, though porous, on heat sensitive materials. A solid oxide fuel cell (SOFC) is an application where porous platinum films have been used.[56]

In the adhesion tests, platinum oxide films grown on soda lime glass, silicon substrate with native oxide and Al_2O_3 or TiO_2 adhesion layers all passed the common tape test indicating good adhesion. Adhesion of the metallic Pt films was not sufficient according to the tape tests.

In conclusion, thermal ALD has been employed for platinum oxide thin film deposition at 120 and 130 °C using $Pt(acac)_2$ and ozone as precursors. At higher deposition temperatures the films became metallic. The pulse lengths had a substantial effect on resistivity of the films, but only a minor effect on the film growth rate. According to XRD the oxide films were amorphous. The ERDA measurements of the film composition were difficult as the platinum oxide reduces easily under an ion beam bombardment. Therefore, the film composition and the impurity contents could only be estimated. Adhesion of the platinum oxide films was good on all tested surfaces. However, the metallic films did not pass the common tape test. Overall, it has been shown that the properties of the platinum oxide films can be tailored and, consequently, the applicability of the process may be wide regardless of the very narrow deposition temperature range. The possibility to reduce platinum oxide easily might be beneficial in making platinum catalyst surfaces or conductive electrodes.

Acknowledgment. Financial support from the Finnish Funding Agency for Technology and Innovation (Tekes) and ASM Microchemistry Ltd. is gratefully acknowledged. Mikko Heikkilä is thanked for his assistance and expertise on XRD and XRR.

CM801187T

(56) Jiang, X.; Huang, H.; Prinz, F. B.; Bent, S. F. *Chem. Mater.* **2008**, *20*, 3897.